LANGMUIR Article
Cite This: Langmuir 2018, 34, 4241−4248
pubs.acs.org/Langmuir

Solid−Liquid Interface Structure of Muscovite Mica in $SrCl_2$ and $BaCl_2$ Solutions

Stelian Pintea,[†,‡] Wester de Poel,[†] Aryan E. F. de Jong,[†,‡] Roberto Felici,[‡,§] and Elias Vlieg*[,†]

[†]Institute for Molecules and Materials, Radboud University, Heyendaalseweg 135, Nijmegen 6525 AJ, The Netherlands
[‡]European Synchrotron Radiation Facility, Grenoble 38043, France
[§]CNR-SPIN, c/o DICII, University of Tor Vergata, Via del Politecnico 1, Rome I-00133, Italy

ABSTRACT: The structure of the solid−liquid interface formed by muscovite mica in contact with two divalent ionic solutions ($SrCl_2$ and $BaCl_2$) is determined using in situ surface X-ray diffraction using both specular and non-specular crystal truncation rods. The 0.5 monolayer of monovalent potassium present at the surface after cleavage is replaced by approximately 0.25 monolayer of divalent ions, closely corresponding to ideal charge compensation within the Stern layer in both cases. The adsorption site of the divalent ions is determined to be in the surface ditrigonal cavities with minor out-of-plane relaxations that are consistent with their ionic radii. The divalent ions are adsorbed in a partly hydrated state (partial solvation sphere). The liquid ordering induced by the presence of the highly ordered crystalline mica is limited to the first 8−10 Å from the topmost crystalline surface layer. These results partly agree with previous studies in terms of interface composition, but there are significant differences regarding the structural details of these interfaces.

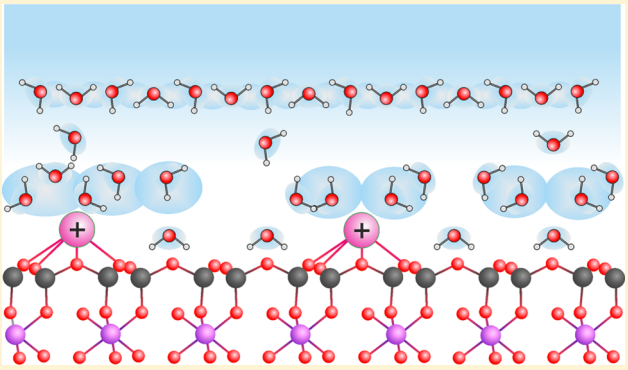

1. INTRODUCTION

Muscovite mica, the most common form of mica, finds many scientific and technological applications derived from its bulk and surface properties. Its atomically flat (001) surface[1] is a perfect substrate for the macromolecular (mono) layers growth[2−5] and the study of DNA.[6,7] It is also often used as a model surface for crude oil−mineral reservoir interaction investigations in order to increase the efficiency of the oil recovery process.[8−11]

When cleaving mica along the (001) plane, the K^+ ions at this plane are distributed evenly over both halves, generating two charge neutral surfaces with each a K^+ coverage of 0.5 monolayer (ML). In contact with an electrochemical solution, these ions can be exchanged by others, both monovalent and divalent.[12−17] This exchange and the details of the charge state at the interface are important for the interaction of the surface with its environment, for example in the case of wetting of oil/water mixtures.[8,11] Divalent ions, the subject of this study, are thought play an important role in enhanced oil recovery using low salinity flooding.[18,19]

The aim of this study is to determine the interface structure of muscovite mica in contact with electrolyte solutions containing divalent cations, $SrCl_2$ and $BaCl_2$. We use surface X-ray diffraction (SXRD) for these in situ structure determinations. Both systems have been studied earlier using X-ray reflectivity (XRR) (including element specific resonant anomalous X-ray reflectivity (RAXR))[14−16] and computer simulations.[20,21] We extend the experimental studies by including a large number of non-specular crystal truncation rods (CTRs), i.e., rods with in-plane momentum transfer, that allow the precise determination the lateral position of the atoms at the interface. The structural details we will address are the presence (or absence) of multiple absorption sites for the cations, the level of charge compensation and lateral ordering in the hydration layers.

2. EXPERIMENTAL DETAILS

SXRD is a well-known method for studying surfaces and (buried) interfaces.[22−24] The modulation of the reflected intensity along the l direction of reciprocal space (thus along the crystal truncation rods, CTRs) is measured as a function of the momentum transfer $Q = h\cdot\vec{a}^* + k\cdot\vec{b}^* + l\cdot\vec{c}^*$, where $\vec{a}^*$, $\vec{b}^*$, and $\vec{c}^*$ are the reciprocal lattice vectors and (hkl) the diffraction indices. For the experimental measurements the vertical z-axis diffractometer of ID03 beamline of the European synchrotron radiation facility (ESRF) was used.[25] A monochromatic X-ray beam with 15 keV energy (λ = 0.8266 Å) and 1 × 0.02 mm^2 size at the sample position was directed at the sample under an incident angle of 0.6° for all the non-specular rods. The diffracted intensities were recorded using a Maxipix 2 × 2 area detector and measurements were performed in a stationary geometry.[26] Structure factor amplitudes were obtained by integrating the diffracted intensities using a specially written script that applies all the necessary correction factors. To account for the non-linear variation of the X-ray

Received: February 13, 2018
Revised: March 20, 2018
Published: March 22, 2018

DOI: 10.1021/acs.langmuir.8b00504
Langmuir 2018, 34, 4241−4248

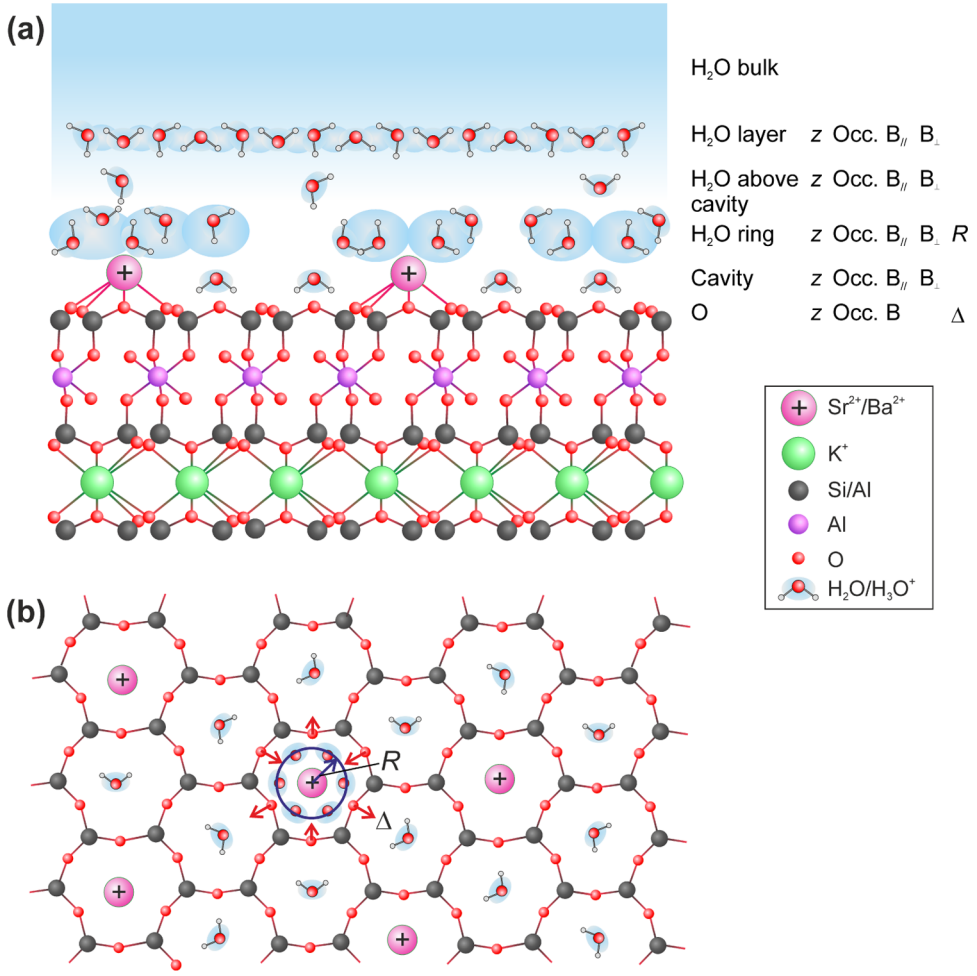

Figure 1. (a) Side and (b) top view of the surface model used for data analysis. In the ditrigonal cavities the divalent ions and water are allowed. Around the cations in the cavity a hydration shell is modeled by rings of twelve oxygen atoms with radius *R*. The model is completed by additional water layers and a continuous film with the density of bulk water. In the top view only the topmost Si/Al and O layers are shown for clarity. The topmost O can be laterally displaced over a distance Δ as indicated by the red arrows.

absorption when passing through the water and mylar foil covering the muscovite mica, an incident and exit angle dependent correction factor was applied during the integration. This correction uses the 13 μm thickness of the mylar foil and an estimated 20 μm for the water/solution film on top of the sample.

High quality muscovite mica sheet, $KAl_2(Si_3Al)O_{10}(OH)_2$, supplied by S&J Trading Inc., Glen Oaks, New York, was cut to pieces of 45 × 45 mm^2. This large sample size was chosen to minimize edge effects and to provide a large flat area for accurate experiments. The unit cell parameters for the monoclinic crystalline lattice ($C2/c$ space group) of muscovite mica are: a = 5.1906 Å, b = 9.008 Å, c = 20.047 Å and β = 95.747°. High purity salts (Sigma-Aldrich codes 439665 and 202738) and ultrapure water (resistivity ≥ 18.2 MΩ·cm) were used for electrolyte solution preparation. A freshly cleaved muscovite piece was immersed for about 20 min in 10^{-2} M aqueous solution of either $SrCl_2$ or $BaCl_2$. After removal from the solution, the sample was placed on the plateau of an environment cell. Additional solution drops were added to the sample surface and to the reservoir of the cell and then mylar foil (13 μm; Lebow Company, Goleta, California), a metal ring and an O-ring were used to seal the surface to prevent it from drying during the experiment. The entire cell was subsequently mounted on the diffractometer. No degradation of the liquid film or the sample surface was noticed during the experiment.

For each sample, first a singly terminated surface area was selected by scanning the (1,1,1.4) reflection that is particularly sensitive in this respect. For details, we refer to previous results.[1,17] We measured 13 different rods and have used an estimated agreement factor[24] of 5% to calculate the experimental error bars.[17] Ideally, the applied geometric correction factors put all rods on the same scale, but we found that adding individual scale factors for each rod gave significantly improved fits.

The data fitting was performed using the ROD software[27] that applies a χ^2 minimization algorithm to the experimental data and a parametrized model comparison. In the calculations the ionic scattering coefficients for Sr^{2+}, Ba^{2+}, and Cl^-, averaged scattering coefficients taking into account the 25% Si/Al bulk substitution and theoretical values of the anomalous dispersion coefficient at 15 keV were used.[28] For the muscovite bulk model the atomic positions from the study of Güven was used.[29] The use of heavy ions of Sr^{2+} and Ba^{2+} facilitates the X-ray analysis owing to their strong scattering power.

3. RESULTS AND DISCUSSION

3.1. Fitting and Surface Models. During the data analysis several models were tried in order to find the one that fits our data best, while being as simple as possible. The model we selected is shown in Figure 1 and is similar to the one we used for monovalent ions,[17] with the main difference that now a continuous water layer with bulk density is included to represent the liquid away from the interface.[30,31] On the right all the free parameters for each atomic layer are listed: z—displacement parameter along the c-axis; occ.—occupancy; $B_{\parallel}$ and $B_{\perp}$—the in-plane and out-of-plane Debye–Waller

DOI: 10.1021/acs.langmuir.8b00504
Langmuir 2018, 34, 4241−4248

Table 1. Determined Structural Parameters of the Muscovite Mica−10^{-2} M $SrCl_2$ Aqueous Solution Interface[a]

element		z-height (Å)	occupancy (ML)	in-plane vibration ($u_{\parallel}$) (Å)	out-of-plane vibration ($u_{\perp}$) (Å)
bulk water		4.3 ± 0.4 (width 0.4 ± 0.2)			
water layer		5.1 ± 0.4	2 ± 1	∞	0.2 ± 0.1
water/Cl^- above cavity		3.7 ± 0.4	0.76 ± 0.05/0.35 ± 0.03	1.2 ± 0.2	0.3 ± 0.1
hydration ring		2.5 ± 0.4	2.6 ± 0.5	0.7 ± 0.1	0.8 ± 0.2
cavity	water	1.73 ± 0.02	0.79 ± 0.02	0.11 ± 0.05	0.11 ± 0.05
	Sr^{2+}	Δz = 0.03 ± 0.02 (with respect to bulk K)	0.21 ± 0.02	0.14 ± 0.05	0.14 ± 0.05
$O_{bulk\text{-}top}$		Δ = −0.03 ± 0.02	≡1	0.12 ± 0.05	0.12 ± 0.05

[a]The zero of the height is the average height of the topmost O atoms of the mica surface.

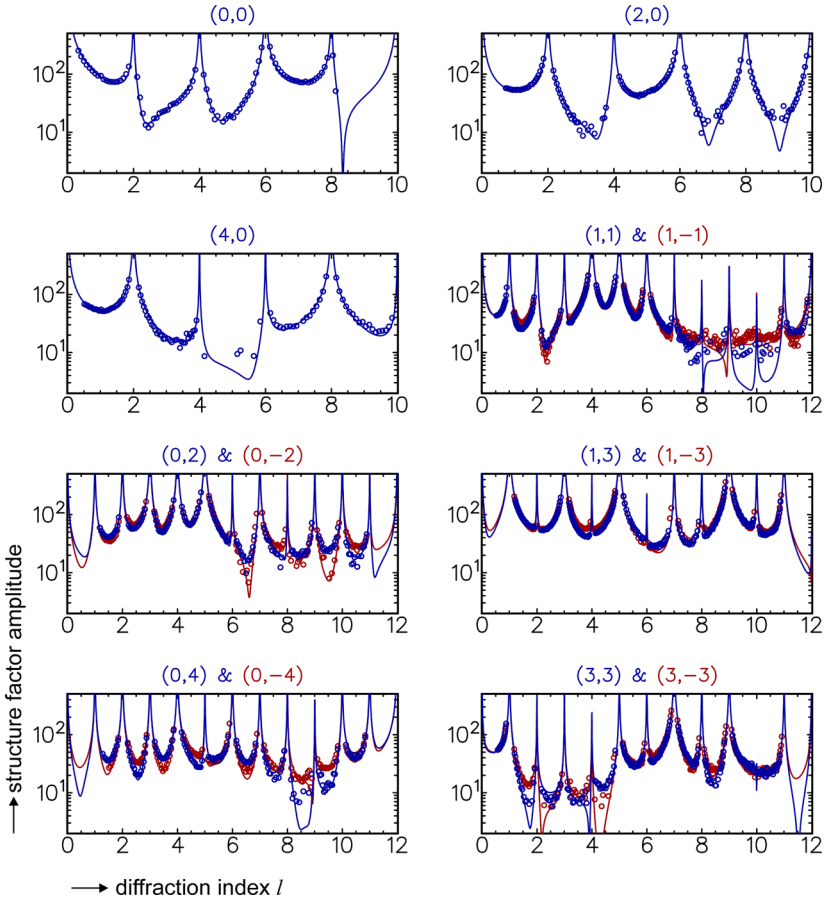

Figure 2. Best fit (solid curves) and the measured crystal truncation rods (circles) for the muscovite mica−$SrCl_2$ solution solid−liquid interface. The plots with the red and blue data plus curves show the rods that are not equivalent because of the singly terminated surface of the muscovite samples.

parameters accounting in our case for the level of ordering as well.[32] Because the scattering of the X-rays from the hydrogen atoms can be neglected, in all cases water molecules were modeled as a single oxygen atom. We find no relaxation in the crystalline muscovite atoms except small values for the topmost layers. The changes in the surface tetrahedral structure are observed through the displacement (Δ) of the topmost oxygen layers presented in Figure 1b by the red arrows.

In the surface cavities we allow either the divalent Sr^{2+} or Ba^{2+} (exchanging the K^+) or water. The sum of the divalent ion and water occupancies in the cavities is fixed at 1, i.e., each cavity is assumed to be occupied (additional water is possible and is modeled using separate layers). After cleavage, ideally speaking, half of the K^+ ions along the cleavage plane will be found on the surface of the sample to maintain charge neutrality (one ion per two ditrigonal cavities). We define 1 monolayer (ML) as a full K^+ layer in the bulk and thus the surface has 0.5 ML K^+ after cleaving. For the divalent ions, a coverage around 0.25 ML is thus expected. Each divalent ion has its occupancy and height as fitting parameters. We also allow the presence of additional atoms located above the cavities, either H_2O or Cl as discussed later.

Around the entities in the cavity a hydration shell was modeled by a hydration ring that is mimicking a uniform charge distribution in the lateral direction (see Figure 1b). The number of (partially occupied) atom positions in the hydration ring was set at 12 to mimic a continuous electron density, because the exact in-plane orientation of the relatively weakly bonded and mobile water molecules is not detectable in this diffraction experiment. The hydration ring is centered on the divalent ion in the cavity and independent out-of-plane displacement, radius, in-plane and out-of-plane Debye−Waller

DOI: 10.1021/acs.langmuir.8b00504
Langmuir 2018, 34, 4241−4248

parameters were used during the data analysis. Initial models contained several rings, but during the data analysis it turned out that one hydration ring is sufficient for a good fit of our data. Since they are located directly at the surface, the divalent ions thus only have approximately half a hydration shell that is modeled here as a hydration ring. In the context of surface adsorption, this configuration has been called inner sphere configuration, in contrast to outer sphere where a full hydration shell is present.[14,21]

The highly ordered crystalline substrate is expected to induce (limited) ordering in the solution film covering it. To account for this, on the top of the already described system, additional water layers are allowed, each modeled by a single water molecule (or, more precisely, a single oxygen atom) per surface unit cell. We find that one layer with only out-of-plane order, thus without lateral order, is sufficient to model the data if the additional bulk solution is modeled by a uniform layer with bulk charge density. This latter layer has its starting height and width as fitting parameters.

Several additional model parameters and variations were tested (e.g., occupancy of the last mica layers, lateral displacements of the divalent ions, divalent ions on top of Si/Al, etc.), but these did not give significant improvements in the fit and were therefore not included in the final model.

During the fitting procedure the surface sensitivity was increased by decreasing the sensitivity for the bulk crystal signal (around the bulk Bragg peaks). This was done by increasing the error bars for the points within 0.3 units along the l direction on each side of these Bragg reflections. The weight of the specular rod was increased by a factor 5 in order to have more sensitivity to layers with only out-of-plane order.

3.2. Structure of Muscovite–$SrCl_2$ Solid–Liquid Interface. The results for the muscovite mica–10^{-2} M $SrCl_2$ solution interface structure are presented in Table 1 and shown in Figures 2 and 3b. There is excellent agreement between data and fit with a normalized χ^2 value for the whole data set (of about 2500 data points) of 1.76. Moreover, the good agreement between the (11) and $(1\bar{1})$ rods proves the accuracy of the single termination selection and assignment. For the discussion we divide the interface in three regions: the crystalline region, the interface region and the liquid region.

The crystalline region is characterized by small to zero relaxations for the topmost four atomic layers of muscovite mica. There is only a minor lateral displacement of the topmost oxygen (Δ = −0.03 Å), confirming the rigid structure of muscovite mica mineral.

The interface region contains the layers with in-plane ordering, i.e., the divalent ions with their hydration shell/ring and the layer containing H_2O or Cl^-. An ideal cleavage and surface charge compensation should lead to a fraction of 0.25 of the surface cavities filled by Sr^{2+}. During the fitting procedure we allowed the presence in the cavity of Sr^{2+} and H_2O at the same height. The Sr^{2+} occupancy obtained was 0.21 ± 0.02, indicating a minor charge under compensation. Computer simulations by Kobayashi et al. indicate that Sr^{2+} could also be located on top of the Al of the topmost mica layer.[21] We therefore also tried such models, but could not obtain a good fit to the data. The hydration ring that represents part of the hydration shell of the Sr^{2+} ions contains 2.6H_2O molecules per ring, with an Sr–O distance of 2.2 ± 0.3 Å. Only one additional layer with limited lateral order is present and is located above the center of the ditrigonal cavity. If we assume it to be H_2O (modeled as O), it would have an occupancy of 0.76 ML. From the location, it could be part of the hydration shell (the distance to Sr would then be 1.9 ± 0.3 Å). However, using XRD we cannot uniquely determine its location with respect to Sr^{2+}, since this ion occupies about one in five cavities and the charge density of the H_2O could equally well be located above a cavity without Sr^{2+}. Moreover, the density could also originate from a Cl^- ion. In that case, owing to the fact that Cl^- is heavier than O, the occupancy would be 0.35 ML. Also a mixture of H_2O and Cl^- cannot be excluded based on the charge density only. Even Sr^{2+} is a theoretical possibility, but this would have a very low occupancy and is not expected so close to the hydration shell of the Sr^{2+} ion that is directly on the surface.

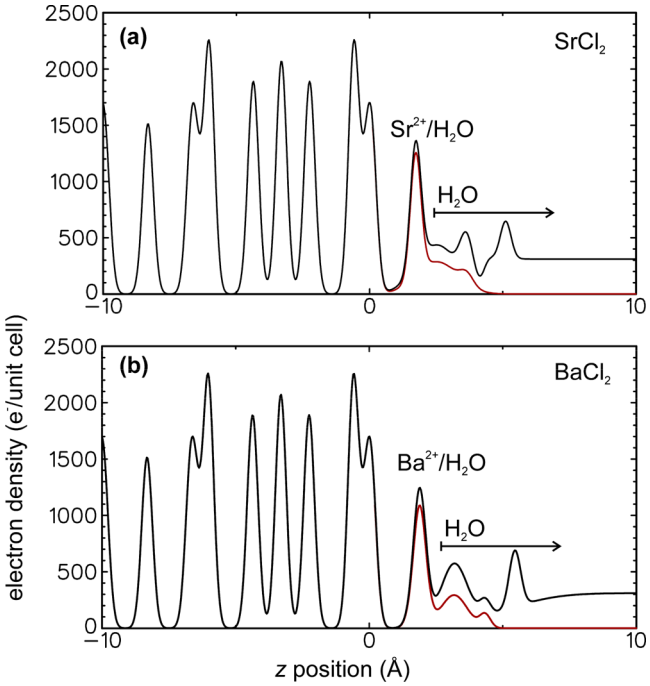

Figure 3. z-Projected electron density as derived from the optimum fit model for (a) $SrCl_2$ and (b) $BaCl_2$. The black curves represent the total density, or (00) Fourier component, the red curves show the density with lateral order using the (11) Fourier component.

The liquid region (without in-plane order) consists of one layer with perpendicular order ("layering") and a film modeled with the bulk density of water. The overall charge density of the model is shown in Figure 3a (black curve). By taking the (11) Fourier component of the charge density, the layers with lateral ordering become visible (red curve). As typical for solid–liquid interfaces, the number of layers with lateral order is less than those with perpendicular order.

3.3. Structure of Muscovite–$BaCl_2$ Solid–Liquid Interface. The results for the muscovite mica–10^{-2} M $BaCl_2$ solid–liquid interface structure are summarized in Table 2 and shown in Figures 4 and 3b. The data set is similar in size (>2800 unique reflections) and gave a normalized χ^2 of 1.32 using the same agreement factor as in the previous data set (5%). As in the case of muscovite mica in $SrCl_2$ solution, no out-of-plane relaxations for the topmost crystalline layers were needed to fit the data. The only modification in the crystalline region is the change in direction of the relaxation of the O atoms (Δ = 0.04 Å). A small enhancement of the vibration parameter of this layer is observed, but it remains at low, solid-like, value: u = 0.16 ± 0.10 Å.

DOI: 10.1021/acs.langmuir.8b00504
Langmuir 2018, 34, 4241–4248

Table 2. Determined Structural Parameters of the Muscovite Mica−10^{-2} M $BaCl_2$ Aqueous Solution Interface

element		z-height (Å)	occupancy (ML)	in-plane vibration ($u_{\parallel}$) (Å)	out-of-plane vibration ($u_{\perp}$) (Å)
bulk water		5.0 ± 0.4 (width 2 ± 1)			
water layer		5.5 ± 0.4	3.4 ± 1	∞	0.2 ± 0.1
water/Cl^- above cavity		4.3 ± 0.4	0.2 ± 0.1/0.08 ± 0.05	0.3 ± 0.1	0.3 ± 0.1
hydration ring		3.2 ± 0.4	1.8 ± 0.5	0.8 ± 0.2	0.8 ± 0.2
cavity	water	1.88 ± 0.02	0.77 ± 0.02	0.5 ± 0.1	0.25 ± 0.08
	Ba^{2+}	Δz = 0.18 ± 0.02 (with respect to bulk K)	0.23 ± 0.02	0.24 ± 0.05	0.24 ± 0.05
$O_{bulk\text{-}top}$		Δ = 0.04 ± 0.02 Å	≡1	0.16 ± 0.05	0.16 ± 0.05

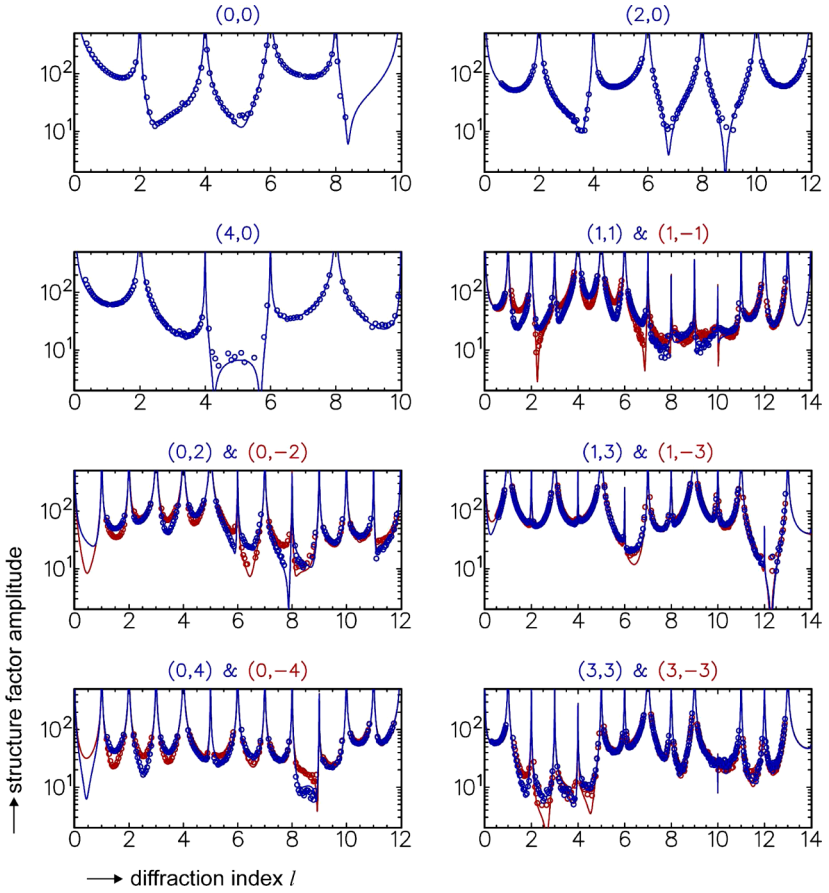

Figure 4. Best fit (solid curves) and the measured crystal truncation rods (circles) for the muscovite mica−$BaCl_2$ solid−liquid interface.

The occupancy for the Ba^{2+} was 0.23 ± 0.02 ML and the rest of the surface cavities is occupied by water (0.77 ± 0.02 ML). Both entities present in these cavities are modeled using the same displacement properties, but with individual vibration parameters. The Ba^{2+} is surrounded by one hydration ring with an occupancy of 1.8 ML and positioned such that the Ba−O distance is 2.7 Å. As in the $SrCl_2$ case, above the hydration ring one atom is located in the center of the ditrigonal cavity. If we assume this is water its occupancy is 0.21 ML and it could be part of the hydration shell around Ba^{2+}. In this case it would be located above the Ba ion at a distance of 2.7 Å. Alternatively, the modeled charge density could be from Cl^- with an occupancy of 0.08 ML and possibly located above sites without Ba^{2+}. The remaining layers are without in-plane order and are modeled as one water layer and a water film with bulk density.

3.4. Discussion. Our analysis is most precise for the well-ordered part of the interface, and for the heavy divalent ions in particular. We find that the Sr^{2+} and Ba^{2+} cations adsorb at the surface ditrigonal cavities of muscovite mica. The previous XRR results were only sensitive to the out-of-plane positions of the atoms, ions, and molecules populating the interface, but they correctly assumed the center of the ditrigonal cavities to be the in-plane adsorption site. Computer simulations by Meleshyn also favor the ditrigonal site for the divalent ions.[20] We find a small difference in the adsorption heights of the two divalent ions: z_{Sr} = 0.03 ± 0.02 Å and z_{Ba} = 0.18 ± 0.02 Å with respect to the position of bulk K^+. The occupancies we find are 0.21 ± 0.02 and 0.23 ± 0.02 ML for Sr and Ba, respectively. These values are quite accurate, because various models with different amounts of fitting parameters always gave very similar results for the position and occupancy of these divalent ions. The tabulated radii[33] for 6-fold coordination for the relevant ions are $r(K^+)$ = 1.38 Å, $r(Sr^{2+})$ = 1.18 Å, and $r(Ba^{2+})$ = 1.35 Å. Based on this, a small inward relaxation of Sr^{2+} is expected. That fact that this is not observed might be explained by changes in the hydration shell of the divalent ions with respect to K^+. Comparing the two divalent ions, the outward relaxation

DOI: 10.1021/acs.langmuir.8b00504
Langmuir 2018, 34, 4241−4248

Table 3. Height and Coverage of the Divalent Ions Adsorbed on Muscovite Mica[a]

	solute	concn (M)	z (Å)	ML
		Sr^{2+}		
this study—SXRD	$SrCl_2$	10^{-2}	1.73 ± 0.02	0.21 ± 0.02
Park et al. (2006)—RAXR	$Sr(NO_3)_2$	10^{-2}	1.26 ± 0.22	0.28 ± 0.12
			4.52 ± 0.24	0.36 ± 0.12
Park et al. (2008)—RAXR	$Sr(NO_3)_2$	10^{-2}		0.20 ± 0.03
Lee et al. (Langmuir, 2010)—RAXR	$Sr(NO_3)_2$	10^{-2}	1.38 ± 0.07	0.26 ± 0.02
			4.58 ± 0.07	0.31 ± 0.02
Lee et al. (Geochim., 2010)—RAXR	$SrCl_2$	10^{-2}	1.32 ± 0.07	0.24 ± 0.02
Meleshyn (2010)—Monte Carlo	Sr^{2+}		1.93* ± 0.02	
			3.9 ± 0.2	
Kobayashi et al. (2017)—Mol. Dyn.	Sr^{2+}		1.60	
			2.74*	
		Ba^{2+}		
this study—SXRD	$BaCl_2$	10^{-2}	1.88 ± 0.02	0.23 ± 0.02
Schlegel et al. (2006)—XRR	$BaCl_2$	10^{-2}	2.02 ± 0.05	
			3.8 ± 0.5	
Lee et al. (2007)—XRR	$BaCl_2$	5×10^{-3}	1.98 ± 0.02	0.22
Meleshyn (2010)—Monte Carlo	Ba^{2+}		2.15* ± 0.03	
			4.17 ± 0.07	
Kobayashi et al. (2017)—Mol. Dyn.	Ba^{2+}		2.07*	
			2.90	

[a]Most of the values refer to the first divalent ion that absorbed in an inner sphere hydration state. If listed, the second value refers to a higher outer sphere hydration location, except for the case of Kabayashi et al., where the second value refers to an inner sphere configuration with a different lateral position. The starred values from the computer simulations indicate the energetically most favorable states.

of Ba^{2+} is expected to be 0.17 Å larger than for Sr^{2+} and this agrees very well with our experimental result of 0.15 ± 0.03 Å.

If we compare these results with the most similar results from the literature, significant differences are noticed, as summarized in Table 3. For Sr^{2+}, four different resonant anomalous X-ray studies have been performed using the same Sr^{2+} concentration (and that have the advantage of being exclusively sensitive to this element).[14,34−36] Only the study by Lee et al.[36] used $SrCl_2$, but the counter ion is not expected to have a significant effect on the Sr^{2+} adsorption. The reported coverage is close to 0.25 ML in all cases, thus for this parameter there is a quite good agreement. This is not the case, however, for the height of the Sr^{2+} ion. While our fit yields 1.73 Å, the other experimental results gave significantly smaller values, with the most recent results reporting about 1.35 Å. While our value corresponds to a small inward relaxation by 0.03 Å with respect to the position of bulk K^+, a height of 1.35 Å yields an inward relaxation of 0.41 Å, which is 2 times the difference in ionic radii. The simulations of Meleshyn[20] and Kobayashi et al.[21] give values that agree better with our experimental value, with a difference of +0.2 and −0.13 Å, respectively, but the difference is still outside the error bars (if reported). In addition, Kobayashi et al. find that a lateral position above the topmost Al atom and a height of 2.74 Å is energetically most favorable, but this strongly disagrees with our experiment.

In our study we find no evidence for additional Sr^{2+} in higher layers (in a fully hydrated state) with significant order or density, unlike the experimental results of Park et al.[14] and Lee et al.[35] Although we tried several different models that include the two adsorption sites for Sr^{2+}, at the end one always gave an occupancy near zero. Our data set with a large number of non-specular rods shows that if such additional Sr^{2+} layers are present, they do not have any lateral order. Since we find that the Sr^{2+} layer in the ditrigonal cavity has a coverage of 0.21 ML and thus almost completely compensates the surface charge, additional Sr^{2+} layers are not expected. The same reasoning makes the presence of significant amounts of Cl^- near the interface unlikely: such ions are only expected if the Sr^{2+} coverage would be such that charge overcompensation occurs. On the other hand, the presence of H_3O^+ or OH^- can change the charge picture completely, while being indistinguishable from H_2O using our method. Caution is thus needed to interpret the densities derived from our fits, especially if we consider the ionizing effects of the X-ray beam.

Figure 5a directly compares the projected electron density across the interface of our $SrCl_2$ study and the most relevant literature. This shows that there is only limited agreement between these studies regarding the structure of the interface. This is not surprising, since the disagreement found for the Sr^{2+} position is expected to be worse for layers that are increasingly disordered.

If we turn to Ba^{2+} (Table 3) we find significantly better agreement for the vertical relaxation between the different studies. The values still differ beyond the various error bars, but agree within about 0.2 Å. This improved agreement with respect to Sr^{2+} is likely caused by the stronger signal from Ba. Nevertheless, the value we find is lower than the other reported values, both experimental and (even more so) computational. It is always difficult to assess the accuracy of the different methods, but our data set with many non-specular rods is particularly sensitive to the location of the well-ordered divalent ions. For example, if we force the Ba^{2+} to be located at a height of 2.00 Å and optimize the other fitting parameters, the χ^2 value goes up by about 70%. This height is thus indeed significantly outside the error bars of our determination. The location of the Ba^{2+} in the center of the ditrigonal cavity agrees fully with the energetically most favorable position as derived from computer simulations.

Layers further removed from the interface, in our case including the hydration ring and additional water layers,

DOI: 10.1021/acs.langmuir.8b00504
Langmuir 2018, 34, 4241−4248

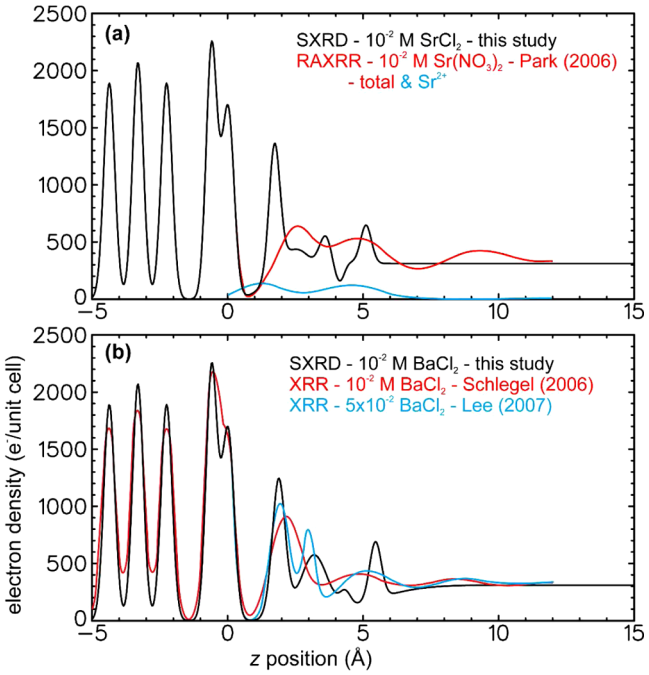

Figure 5. Comparison of the z-projected electron density from this study and from the literature for (a) Sr^{2+} and (b) Ba^{2+}. Park et al.[14] used resonance anomalous X-ray reflectivity, while Schlegel et al.[15] and Lee at al.[16] used X-ray reflectivity.

become increasingly disordered and thus also increasingly more difficult to accurately locate. Figure 5b compares the z-projected electron density we derive from our model with the literature. Compared to the case of Sr^{2+} the agreement is somewhat better, but still not good. This situation is similar to the one found for muscovite in CsCl and RbBr aqueous solution.[17]

Atomic force microscopy has reached a stage in which atomic resolution can be achieved at similar solid−liquid interfaces.[37−39] No studies using the current systems have been reported yet, but such data would help to gain a more complete understanding of the physical chemistry and local structure at such interfaces.

4. CONCLUSIONS

This study precisely determines the adsorption site for two divalent ions on muscovite mica. The Sr^{2+} replaces the K^+ at almost the same (bulk) height: $\Delta z = 0.03 \pm 0.02$ Å while Ba^{2+} has a vertical relaxation of $\Delta z = 0.18 \pm 0.02$ Å. Although the ionic radii of the two divalent ions are slightly smaller than the ionic radius of K^+, their adsorption site is still at higher positions from the topmost crystalline oxygen layer, which could be caused by the (only) partial dehydration of the divalent ions during the adsorption/exchange process. The lateral position of the adsorbed ions is determined to be in the center of the ditrigonal surface cavities. We also find evidence of structuring of the hydration water at the interface. The ordering in the solution is limited to less than 10 Å from the topmost oxygen layer of the crystalline muscovite. Additional divalent or Cl^- ions near the interface are only consistent with our data if present in small amounts and strongly disordered.

There is only limited agreement between the various studies of these systems, in particular for the more disordered layers near the interface. This means that even for such a well-behaved system as muscovite mica, accurately determining the interface structure of a solid−liquid interface remains challenging, both experimentally and computationally.

AUTHOR INFORMATION

Corresponding Author

*E-mail: e.vlieg@science.ru.nl.

ORCID

Wester de Poel: 0000-0002-4077-7231
Roberto Felici: 0000-0001-9897-5866
Elias Vlieg: 0000-0002-1343-4102

Notes

The authors declare no competing financial interest.

ACKNOWLEDGMENTS

We thank the ESRF and the beam line staff for our use of the facilities of ID03.

REFERENCES

(1) de Poel, W.; Pintea, S.; Drnec, J.; Carla, F.; Felici, R.; Mulder, P.; Elemans, J.; van Enckevort, W. J. P.; Rowan, A. E.; Vlieg, E. Muscovite mica: Flatter than a pancake. *Surf. Sci.* **2014**, *619*, 19−24.

(2) Peanasky, J.; Schneider, H. M.; Granick, S.; et al. Self-assembled monolayers on mica for experiments utilizing the surface force apparatus. *Langmuir* **1995**, *11*, 953.

(3) Lowack, K.; Helm, C. A. Polyelectrolyte Monolayers at the Mica/Air Interface: Mechanically Induced Rearrangements and Monolayer Annealing. *Macromolecules* **1995**, *28*, 2912.

(4) van den Bruele, F. J.; De Poel, W.; Sturmans, H. W. M.; Pintea, S.; de Gelder, R.; Wermeille, D.; Juricek, M.; Rowan, A. E.; van Enckevort, W. J. P.; Vlieg, E. Monolayer and aggregate formation of a modified phthalocyanine on mica determined by a delicate balance of surface interactions. *Surf. Sci.* **2012**, *606*, 830−835.

(5) de Poel, W.; et al. Dibenzo-crown-ether layer formation on muscovite mica. *Langmuir* **2014**, *30*, 12570−12577.

(6) Pastré, D.; Hamon, L.; Mechulam, A.; Sorel, I.; Bacconnais, S.; Curmi, P. A.; Le Cam, E.; Pietrement, O. Atomic Force Microscopy Imaging of DNA under Macromolecular Crowding Conditions. *Biomacromolecules* **2007**, *8*, 3712−3717.

(7) Tang, T. C.; Amadei, C. A.; Thomson, N. H.; Chiesa, M. Ion Exchange and DNA Molecular Dip Stick: Studying the Nanoscale Surface Wetting of Muscovite Mica. *J. Phys. Chem. C* **2014**, *118*, 4695−4701.

(8) Drummond, C.; Israelachvili, J. N. Fundamental studies of crude oil-surface water interactions and its relationship to reservoir wettability. *J. Pet. Sci. Eng.* **2004**, *45*, 61−81.

(9) Lord, D. L.; Buckley, J. S. An AFM study of the morphological features that affect wetting at crude oil-water-mica interface. *Colloids Surf., A* **2002**, *206*, 531−546.

(10) Buckley, J. S.; Lord, D. L. Wettability and morphology of mica surfaces after exposure to crude oil. *J. Pet. Sci. Eng.* **2003**, *39*, 261−273.

(11) Haagh, M. E. J.; Siretanu, I.; Duits, M. H. G.; Mugele, F. Salinity-Dependent Contact Angle Alteration in Oil/Brine/Silicate Systems: the Critical Role of Divalent Cations. *Langmuir* **2017**, *33*, 3349−3357.

(12) Gaines, G. L. The ion-exchange properties of muscovite mica. *J. Phys. Chem.* **1957**, *61*, 1408−1413.

(13) Xu, L.; Salmeron, M. An XPS and scanning polarization force microscopy study of the exchange and mobility of surface ions on mica. *Langmuir* **1998**, *14*, 5841−5844.

(14) Park, C.; Fenter, P. A.; Nagy, K. L.; Sturchio, N. C. Hydration and Distribution of Ions at the Mica-Water Interface. *Phys. Rev. Lett.* **2006**, *97*, No. 016101.

(15) Schlegel, M. L.; Nagy, K. L.; Fenter, P.; Cheng, L.; Sturchio, N. C.; Jacobsen, S. D. Cation sorption on the muscovite (001) surface in

DOI: 10.1021/acs.langmuir.8b00504
Langmuir 2018, 34, 4241−4248

chloride solutions using high-resolution X-ray reflectivity. *Geochim. Cosmochim. Acta* **2006**, *70*, 3549−3565.
(16) Lee, S. S.; Nagy, K. L.; Fenter, P. Distribution of barium and fulvic acid at the mica-solution interface using in-situ X-ray reflectivity. *Geochim. Cosmochim. Acta* **2007**, *71*, 5763−5781.
(17) Pintea, S.; De Poel, W.; de Jong, A. E. F.; van der Asdonk, P.; Drnec, J.; Balmes, O.; Isern, I.; Dufrane, T.; Felici, R.; Vlieg, E.; et al. Solid-liquid interface structure of muscovite mica in CsCl and RbBr solutions. *Langmuir* **2016**, *32*, 12955−12965.
(18) Austad, T.; Rezaeidoust, A.; Puntervold, T. Chemical Mechanism of Low Salinity Water Flooding in Sandstone Reservoirs. In *SPE Improved Oil Recovery Symposium*; Society of Petroleum Engineers: Tulsa, OK, 2010.
(19) Sorbie, K. S.; Collins, I. R. A Proposed Pore-Scale Mechanism for How Low Salinity Waterflooding Works. In *SPE Improved Oil Recovery Symposium*; Society of Petroleum Engineers: Tulsa, OK, 2010.
(20) Meleshyn, A. Adsorption of Sr2+ and Ba2+ at the cleaved mica-water interface: free energy profiles and interfacial structure. *Geochim. Cosmochim. Acta* **2010**, *74*, 1485−1497.
(21) Kobayashi, K.; Liang, Y.; Murata, S.; Matsuoka, T.; Takahashi, S.; Nishi, N.; Sakka, T. Ion distribution of hydration structure in the Stern layer on muscovite surface. *Langmuir* **2017**, *33*, 3892−3899.
(22) Feidenhans'l, R. Surface structure determination by X-ray diffraction. *Surf. Sci. Rep.* **1989**, *10*, 105−188.
(23) Robinson, I. K.; Tweet, D. J. Surface X-ray diffraction. *Rep. Prog. Phys.* **1992**, *55*, 599−651.
(24) Vlieg, E. X-ray Diffraction from Surfaces and Interfaces. In *Surface and Interface Science*; Wandelt, K., Ed.; Wiley, 2012; Vol. *1*, pp 375−425.
(25) Balmes, O.; van Rijn, R.; Wermeille, D.; Resta, A.; Petit, L.; Isern, I.; Dufrane, T.; Felici, R. The ID03 surface diffraction beamline for in-situ and real-time X-ray investigations of catalytic reactions at surfaces. *Catal. Today* **2009**, *145*, 220−226.
(26) Vlieg, E. Integrated intensities using a six-circle surface X-ray diffractometer. *J. Appl. Crystallogr.* **1997**, *30*, 532−543.
(27) Vlieg, E. ROD, a program for surface crystallography. *J. Appl. Crystallogr.* **2000**, *33*, 401−405.
(28) Cromer, D. T.; Liberman, D. A. Anomalous dispersion calculations near near to and on the long-wavelength side of an absorption edge. *Acta Crystallogr., Sect. A: Found. Adv.* **1981**, *37*, 267.
(29) Güven, N. The crystal structure of 2M1 phengite and 2M1 muscovite. *Z. Kristallogr. Cryst. Mater.* **1971**, *134*, 196.
(30) Chason, E.; Mayer, T. M. Thin film and surface characterization by specular X-ray reflectivity. *Crit. Rev. Solid State Mater. Sci.* **1997**, *22*, 1−67.
(31) Fenter, P. A. X-ray Reflectivity as a Probe of Mineral-Fluid Interfaces: A User Guide. *Rev. Mineral. Geochem.* **2002**, *49*, 149−221.
(32) Reedijk, M. F.; Arsic, J.; Hollander, F. F. A.; de Vries, S. A.; Vlieg, E. Liquid order a the interface of KDP crystals with water: evidence for icelike layers. *Phys. Rev. Lett.* **2003**, *90*, No. 066103.
(33) Shannon, R. D. Revised Effective Ionic Radii and Systematic Studies on Interatomic Distances in Halides and Chalcogenides. *Acta Crystallogr., Sect. A: Found. Adv.* **1976**, *32*, 751−767.
(34) Park, C.; Fenter, P.; Sturchio, N. C.; Nagy, K. L. Thermodynamics, interfacial structure, and pH hysteresis of Rb2+ and Sr2+ adsorption at the muscovite (001) - solution interface. *Langmuir* **2008**, *24*, 13993−14004.
(35) Lee, S. S.; Fenter, P.; Park, C.; Sturchio, N. C.; Nagy, K. L. Hydrated cation speciation at the muscovite (001) - water interface. *Langmuir* **2010**, *26*, 16647−16651.
(36) Lee, S. S.; Park, C.; Fenter, P.; Sturchio, N. C.; Nagy, K. L. Competitive adsorption of strontium and fulvic acid at the muscovite−solution interface observed with resonant anomalous X-ray reflectivity. *Geochim. Cosmochim. Acta* **2010**, *74*, 1762−1776.
(37) Kimura, K.; Ido, S.; Oyabu, N.; Kobayashi, K.; Hirata, Y.; Imai, T.; Yamada, H. Visualizing water molecule distribution by atomic force microscopy. *J. Chem. Phys.* **2010**, *132*, No. 194705.
(38) Ricci, M.; Spijker, P.; Voitchovsky, K. Water-induced correlation between single ions imaged at the solid-liquid interface. *Nat. Commun.* **2014**, *5*, No. 4400.
(39) Martin-Jimenez, D.; Garcia, R. Identification of Single Adsorbed Cations on Mica−Liquid Interfaces by 3D Force Microscopy. *J. Phys. Chem. Lett.* **2017**, *8*, 5707−5711.

DOI: 10.1021/acs.langmuir.8b00504
Langmuir 2018, 34, 4241−4248